Supporting Information for

Positional isomeric chemosensors: fluorescent and colorimetric cyanide detection based on Si–O cleavage

Yayun Chen, Luting Zhao, Hanghai Fu, Caihui Rao, Zheyao Li and Chuanxiang Liu *

School of Chemical and Environmental Engineering, Shanghai Institute of Technology, Shanghai 201418, China

e-mail: cxliu@sit.edu.cn;

Contents of Supporting Information

1. ^{1}H-NMR spectrum of the mixture of isomers **1** and isomers **2** 2

2. ^{1}H-NMR, ^{13}C-NMR, IR and HRMS-ESI spectrum of the compound *trans*-**3.** 3

3. ^{1}H-NMR, ^{13}C-NMR, IR and HRMS-ESI spectrum of the compound *cis*-**3**.....5

4. UV-vis spectra of titration of *cis*-**3** and *trans*-**3** with TBAF and Na_2S in CH_3CN-H_2O solution. .7

5. UV-vis titration of *cis*-**3** and *trans*-**3** with NaCN in CH_3CN-H_2O solution. 8

6. UV-vis titration of *cis*-**3** and *trans*-**3** with CN^- in CH_3CN. 8

7. UV-vis interference experiments of *trans*-**3** and *cis*-**3** toward CN^- ions. 9

8. Influence of pH on the absorbance of *cis*-**3** and *trans*-**3** 10

9. Emission spectra of titration of *cis*-**3** and *trans*-**3** with TBAF and Na_2S in CH_3CN-H_2O solution. 11

10. Emission interference experiments of *trans*-**3** and *cis*-**3** toward CN^- ions. 12

11. Emission spectra of titration of *cis*-**3** and *trans*-**3** with CN^- in CH_3CN. 12

12. The fluorescence detection limit of *tran*-**3** and *cis*-**3** with CN^- in CH_3CN-H_2O solution. 13

13. ^{1}H NMR titration spectra of isomer **3** with TBACN.....15

14. The final state of ^{1}H NMR titration spectra of isomer **3** with TBACN.....16

15. The fluoride interference experiments on the test paper 16

1. ^{1}H-NMR spectrum of the mixture of isomers 1 and isomers 2

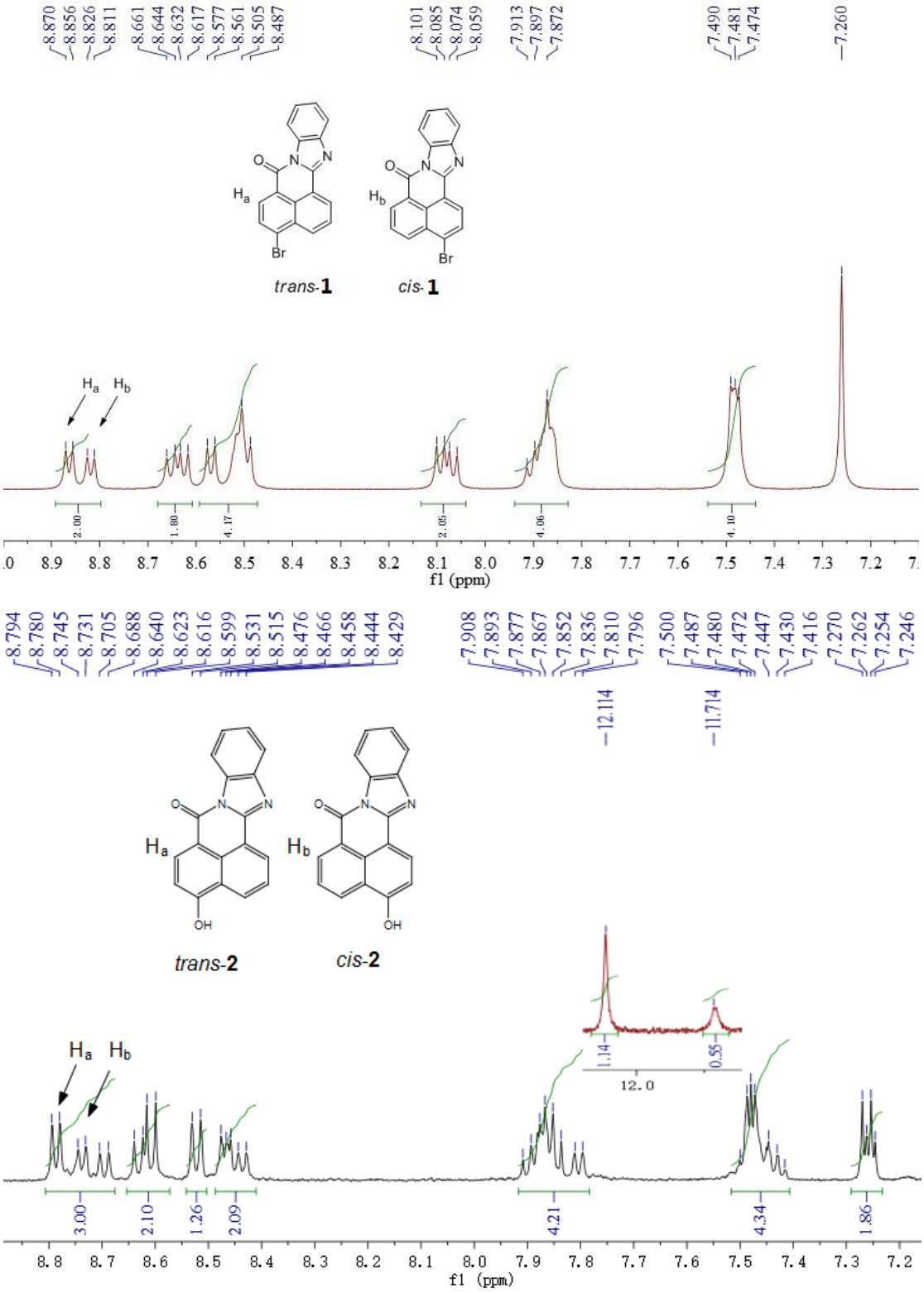

Figure S1. ^{1}H-NMR spectrum of the mixture of isomers **1** ($CDCl_3$, 500 MHz) and **2** (DMSO-d_6, 500 MHz)

2. ^{1}H-NMR, ^{13}C-NMR, IR and HRMS-ESI spectrum of the compound *trans*-3.

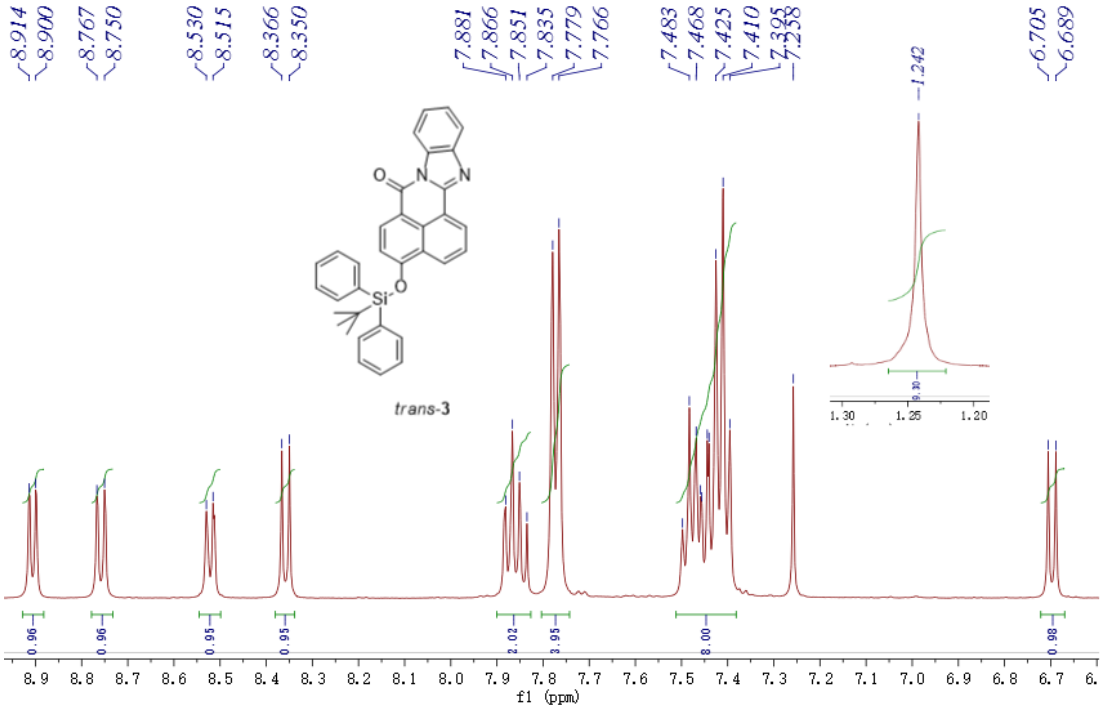

Figure S2. ^{1}H-NMR ($CDCl_3$, 500 MHz) spectrum of compound *trans*-**3**

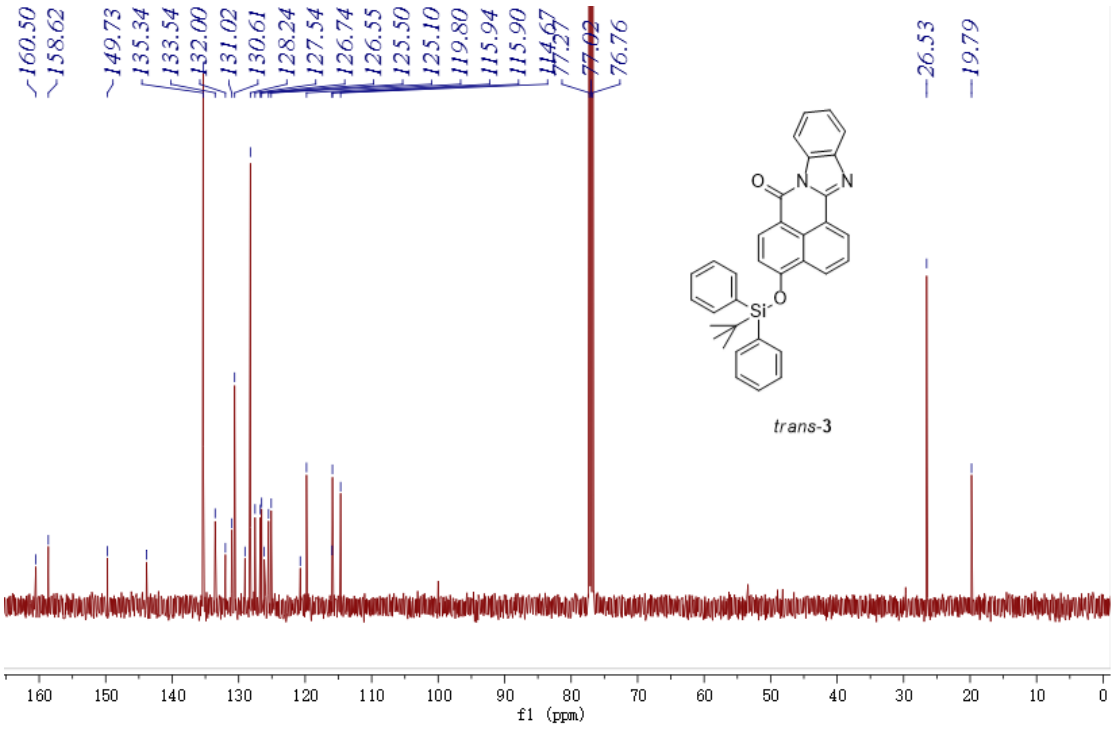

Figure S3. ^{13}C-NMR ($CDCl_3$, 125 MHz) spectrum of compound *trans*-**3**

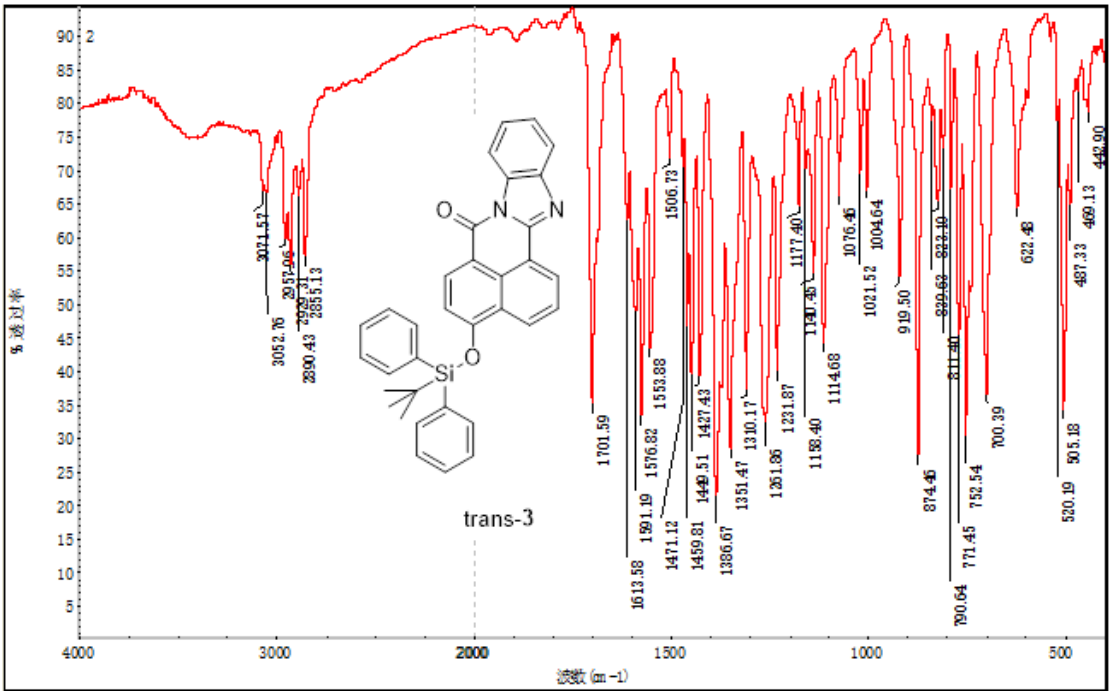

Figure S4. IR spectrum of compound *trans*-**3**

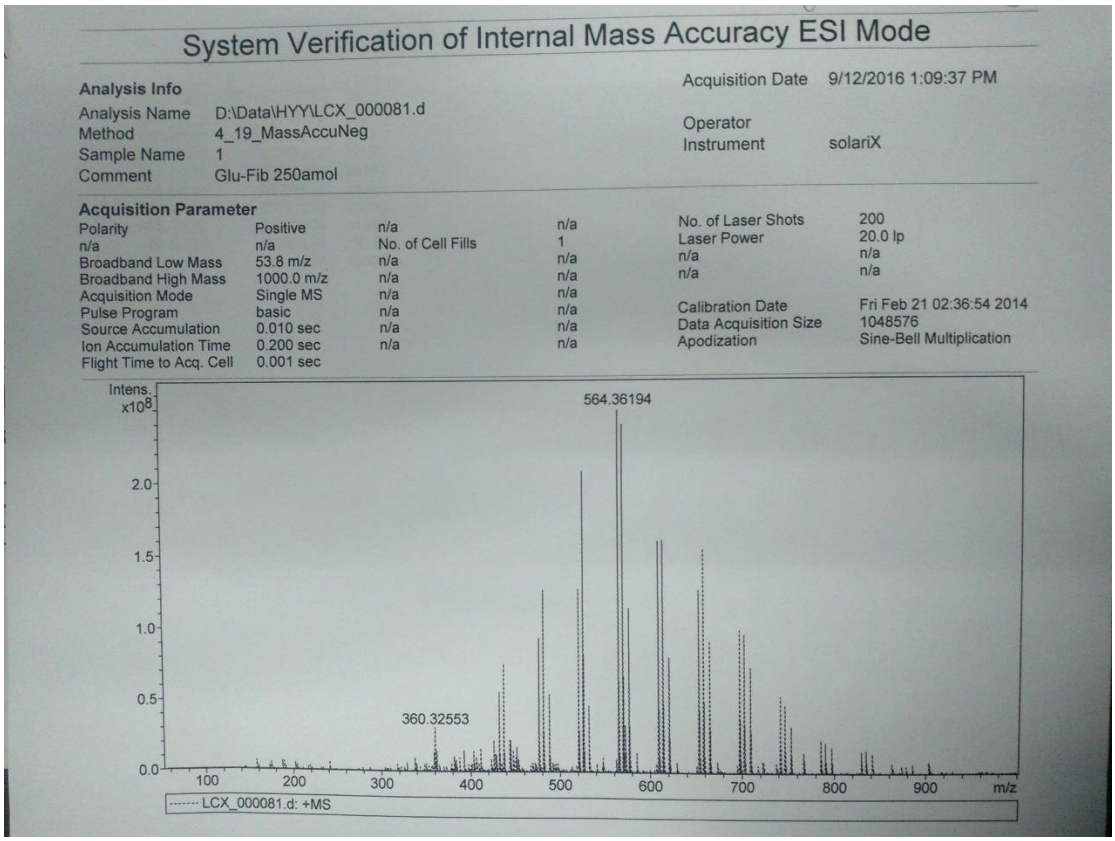

Figure S5. HRMS-ESI mass spectrum of compound *trans*-**3**

3. ^{1}H-NMR, ^{13}C-NMR, IR and HRMS-ESI spectrum of the compound *cis*-3.

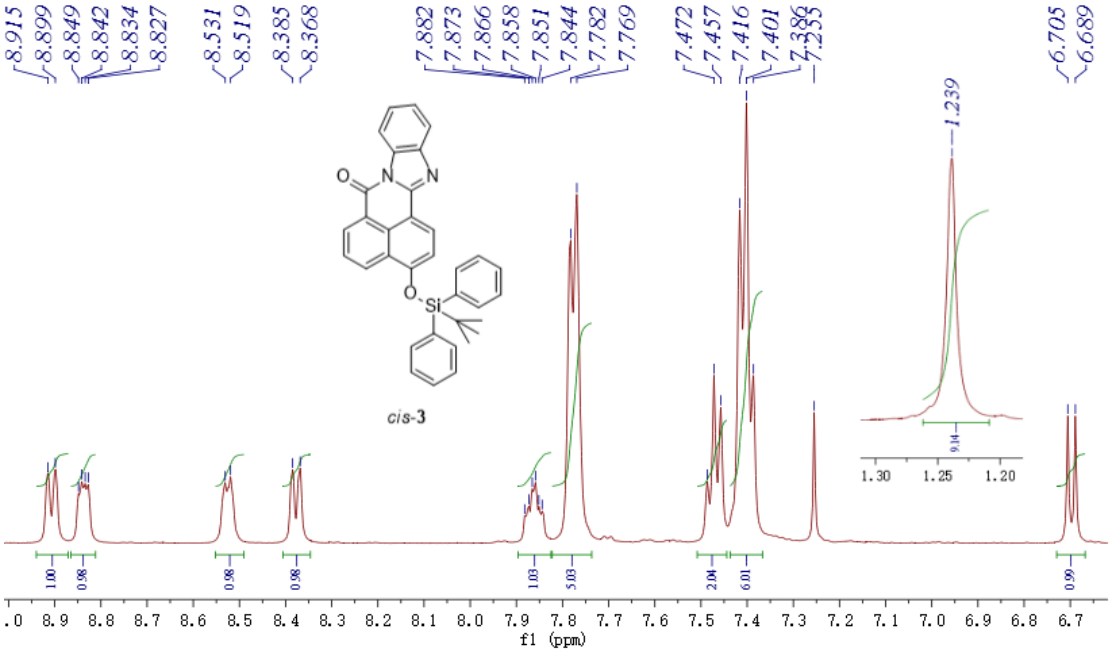

Figure S6. ^{1}H-NMR ($CDCl_3$, 500 MHz) spectrum of compound *cis*-**3**

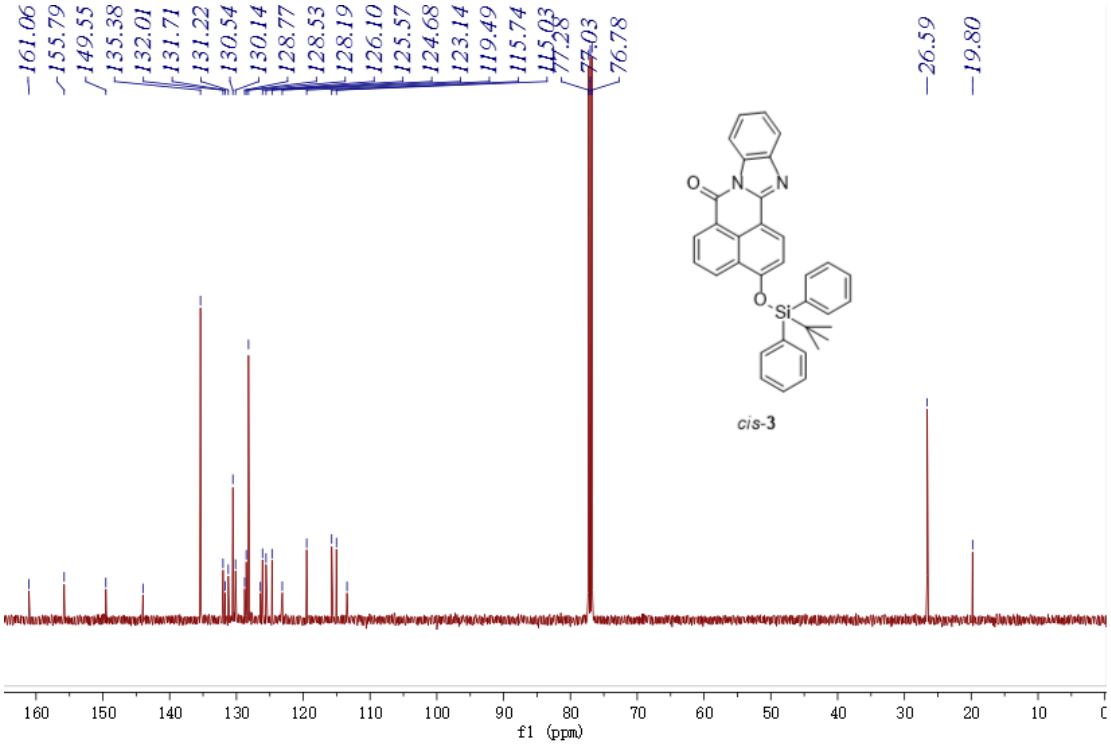

Figure S7. ^{13}H-NMR ($CDCl_3$, 125 MHz) spectrum of compound *cis*-**3**

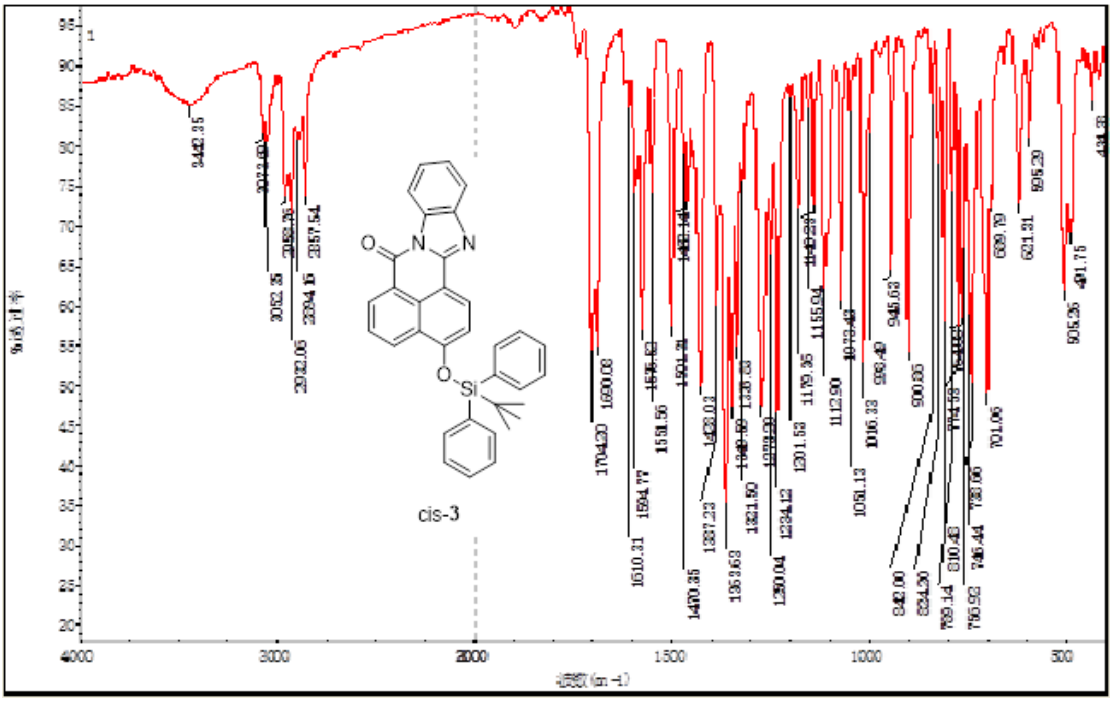

Figure S8. IR spectrum of compound *cis*-**3**

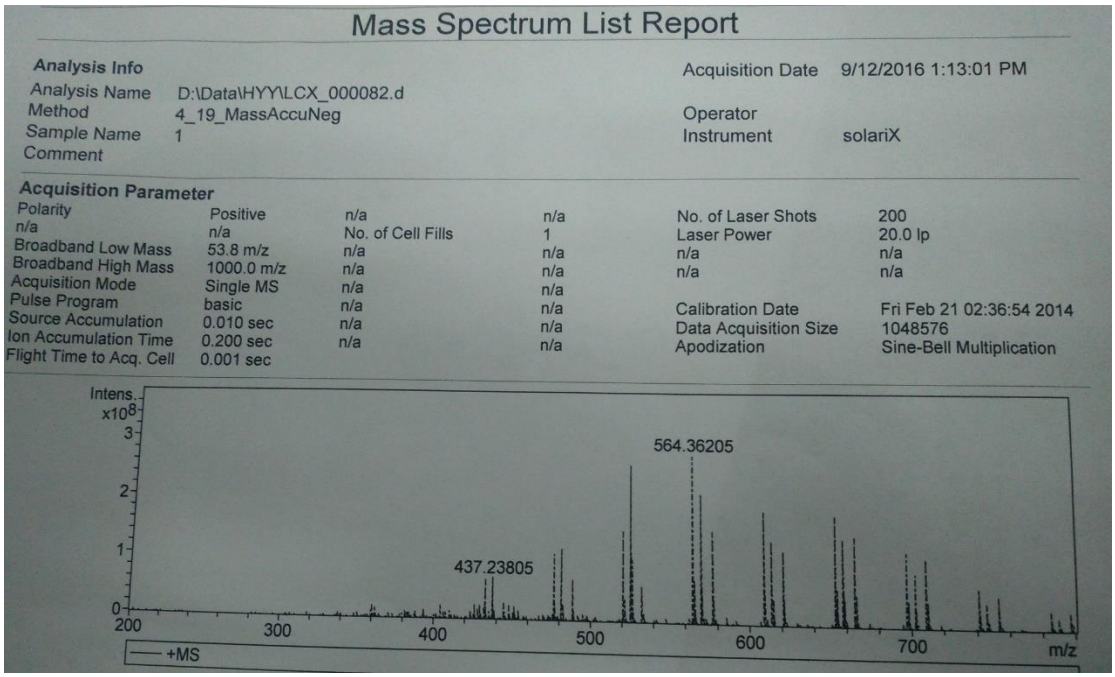

Figure S9. HRMS-ESI mass spectrum of compound *cis*-**3**

4. UV-vis spectra of titration of *cis*-3 and *trans*-3 with TBAF and Na_2S in CH_3CN-H_2O solution.

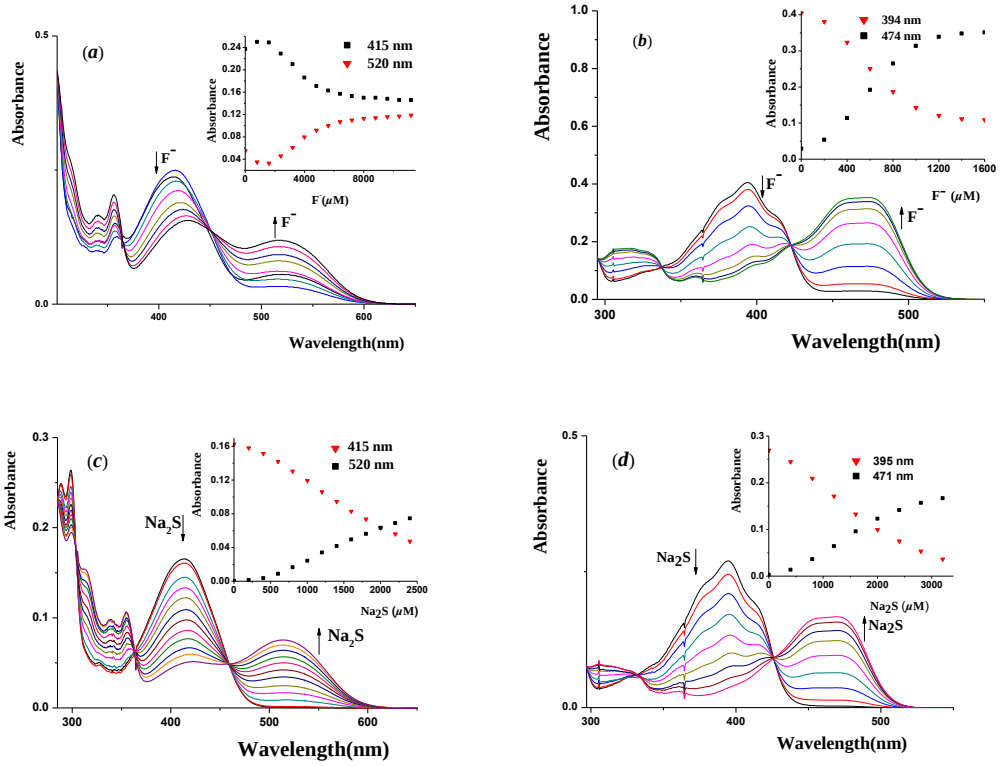

Figure S10. (a) UV-visible titration of *cis*-**3** (20 μM) with TBAF (0 to 120.0 equiv.) in CH_3CN/H_2O (9:1, v/v). The inset shows the absorbance at 415 nm and 520 nm as a function of F^-. (b) UV-visible titration of *trans*-**3** (20 μM) with TBAF (0 to 80.0 equiv.) in CH_3CN/H_2O (9:1, v/v). The inset shows the absorbance at 394 nm and 474 nm as a function of F^-. (c) UV-visible titration of *cis*-**3** (20 μM) with Na_2S (0 to 50.0 equiv.) in CH_3CN/H_2O (9:1, v/v). The inset shows the absorbance at 415 nm and 520 nm as a function of Na_2S. (d) UV-visible titration of *trans*-**3** (20 μM) with Na_2S (0 to 120.0 equiv.) in CH_3CN/H_2O (4:1, v/v). The inset shows the absorbance at 395 nm and 471 nm as a function of Na_2S.

5. UV-vis titration of *cis*-3 and *trans*-3 with NaCN in CH_3CN-H_2O solution.

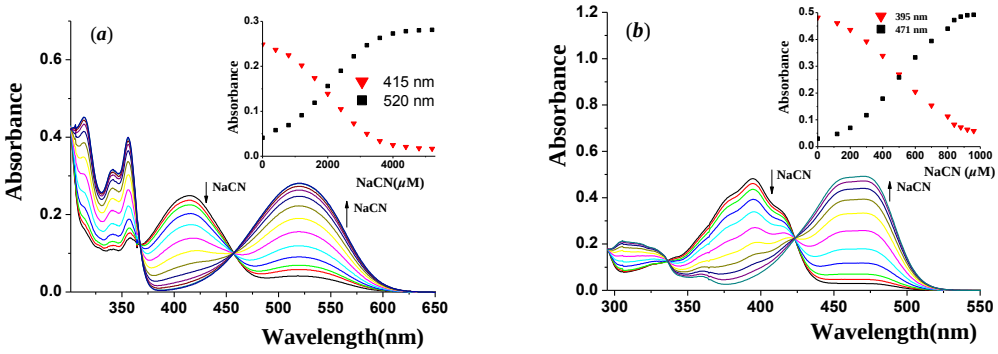

Figure S11. (*a*) UV-visible titration of *cis*-**3** (20 μM) with NaCN (0 to 60.0 equiv.) in CH_3CN/H_2O (9:1, v/v). The inset shows the absorbance at 415 nm and 520 nm as a function of NaCN. (*b*) UV-visible titration of *trans*-**3** (20 μM) with NaCN (0 to 46.0 equiv.) in CH_3CN/H_2O (4:1, v/v). The inset shows the absorbance at 395 nm and 471 nm as a function of NaCN.

6. UV-vis titration of *cis*-3 and *trans*-3 with CN^- in CH_3CN.

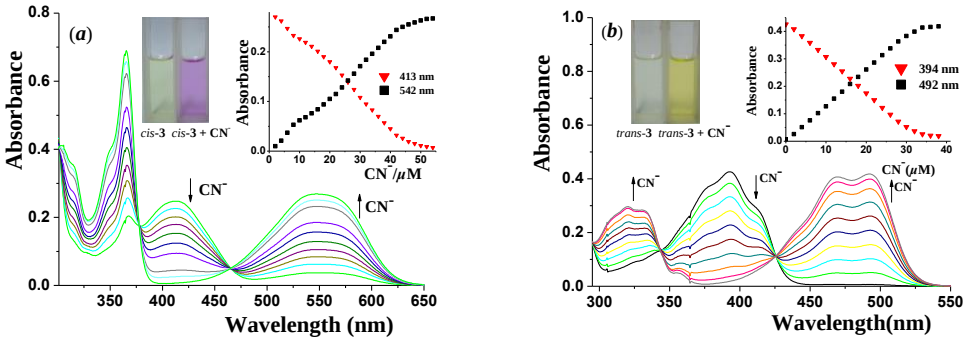

Figure S12. (*a*) UV-visible titration of *cis*-**3** (20 μM) with TBACN (0 to 2.6 equiv.) in CH_3CN. The inset shows the absorbance at 413 nm and 542 nm as a function of [CN^-]. (*b*) UV-visible titration of *trans*-**3** (20 μM) with TBACN (0 to 1.7 equiv.) in CH_3CN. The inset shows the absorbance at 393 nm and 492 nm as a function of [CN^-].

7. UV-vis interference experiments of *trans*-3 and *cis*-3 toward CN^- ions.

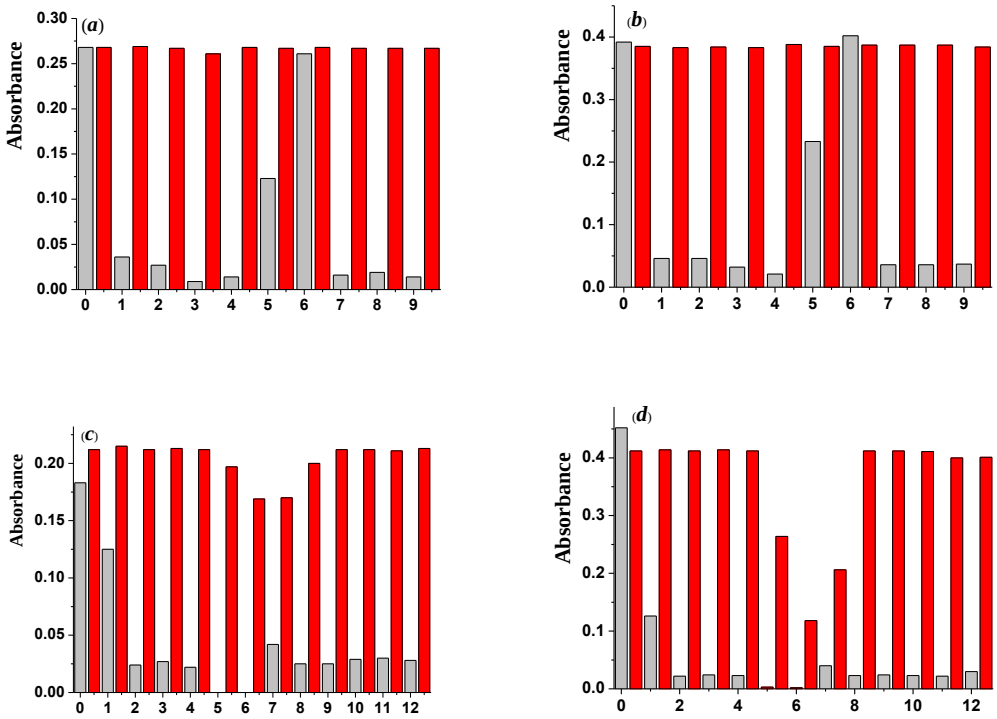

Figure S13. (*a*) Interference experiments of dosimeter *cis*-**3** (20 μM) in CH_3CN for CN^- in the presence of other anions. The gray bars represent the emission at 542 nm of **cis-3** in the presence of 2.6 equiv. of the anion of interest (from 0 to 9: F^-, Cl^-, Br^-, I^-, HSO_4^-, $H_2PO_4^-$, AcO^-, BF_4^-, NO_3^-, ClO_4^-). The red bars indicate the change that occurs upon subsequent addition of 2.6 equiv. of CN^- to the solution containing *cis*-**3** and the anion of interest; (*b*) Interference experiments of dosimeter *trans*-**3** (20 μM) in CH_3CN for CN^- in the presence of other anions. The gray bars represent the emission at 542 nm of *trans*-**3** in the presence of 1.7 equiv. of the anion of interest (from 0 to 9: F^-, Cl^-, Br^-, I^-, HSO_4^-, $H_2PO_4^-$, AcO^-, BF_4^-, NO_3^-, ClO_4^-). The red bars indicate the change that occurs upon subsequent addition of 1.7 equiv. of CN^- to the solution containing *trans*-**3** and the anion of interest; (*c*) Interference experiments of dosimeter *cis*-**3** (20 μM) in CH_3CN/H_2O (9: 1, v/v) for CN^- in the presence of other anions. The gray bars represent the emission at 520 nm of **cis-3** in the presence of 42.0 equiv. of the anion of interest (from 0 to 10: NaCN, F^-, Cl^-, Br^-, I^-, HSO_4^-, $H_2PO_4^-$, AcO^-, BF_4^-, NO_3^-, ClO_4^- , NaSCN, Na_2S). The red bars indicate the change that occurs upon subsequent addition of 42.0 equiv. of CN^- to the solution containing *cis*-**3** and the anion of interest; (*d*) Interference experiments of dosimeter *trans*-**3** (20

μM) in CH_3CN/H_2O (4: 1, v/v) for CN^- in the presence of other anions. The gray bars represent the emission at 471 nm of **trans-3** in the presence of 40.0 equiv. of the anion of interest (from 0 to 10: NaCN, F^-, Cl^-, Br^-, I^-, HSO_4^-, $H_2PO_4^-$, AcO^-, BF_4^-, NO_3^-, ClO_4^-, NaSCN, Na_2S). The red bars indicate the change that occurs upon subsequent addition of 40.0 equiv. of CN^- to the solution containing *trans*-**3** and the anion of interest.

8. Influence of pH on the absorbance of *cis*-3 and *trans*-3

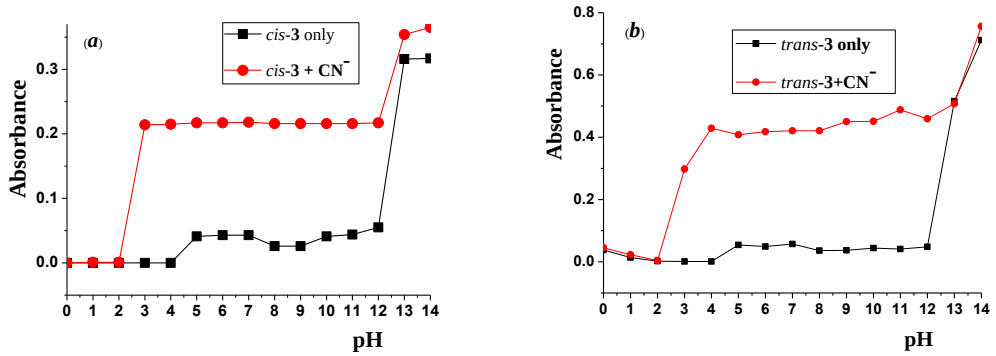

Figure S14. (*a*) Influence of pH on the absorbance at 520 nm of *cis*-**3** and *cis*-**3**+CN^- in CH_3CN/H_2O (9 : 1, v/v); (*b*) Influence of pH on the absorbance at 471 nm of *trans*-**3** and *trans*-**3**+CN^- in CH_3CN/H_2O (4 : 1, v/v).

9. Emission spectra of titration of *cis*-3 and *trans*-3 with TBAF and Na_2S in CH_3CN-H_2O solution.

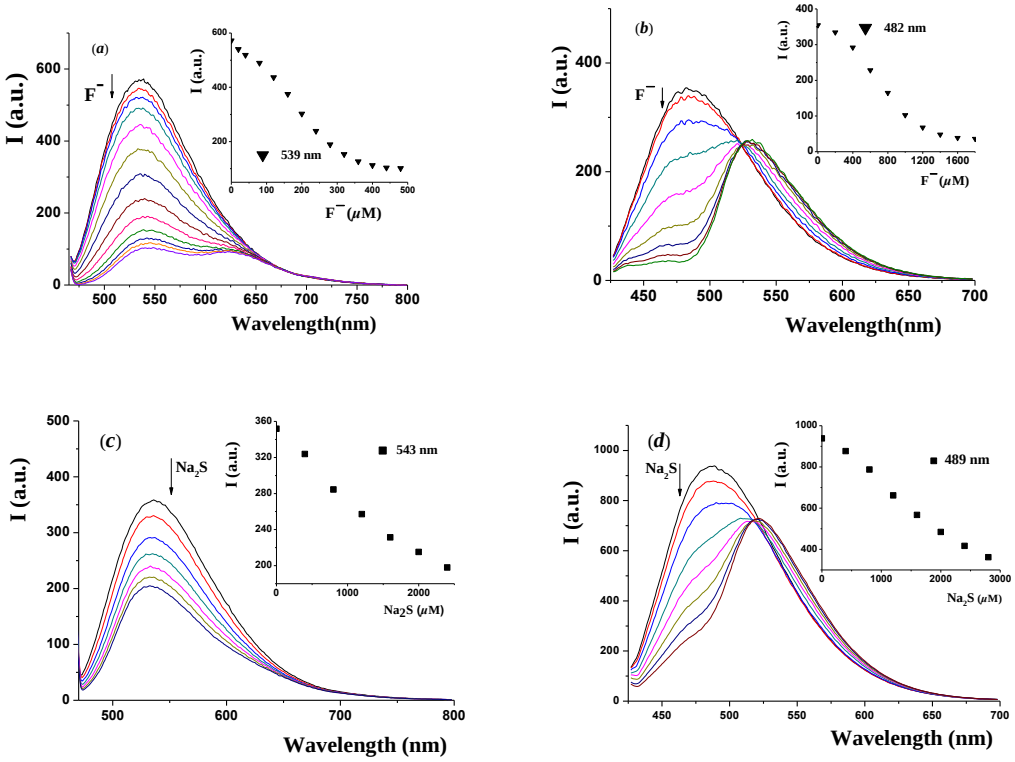

Figure S15. (a) Emission spectra of *cis*-**3** (20 μM, λ_{ex} = 460 nm, in CH_3CN/H_2O (95:5, v/v)) upon addition of increasing concentrations of F^- (as its TBA salt, 0 to 22.0 equiv.). Inset: Plot of emission intensity (λ_{em} = 539 nm) versus TBAF concentration. (b) Emission spectra of *trans*-**3** (20 μM, λex =423 nm, in CH_3CN/H_2O (9:1，v/v)) upon addition of increasing concentrations of F^- (as its TBA salt, 0 to 80.0 equiv.). Inset: Plot of emission intensity (λem = 482 nm) versus TBAF concentration. (c) Emission spectra of *cis*-**3** (20 μM, λ_{ex} =461 nm, in CH_3CN/H_2O (9:1, v/v)) upon addition of increasing concentrations of Na_2S (0 to 120.0 equiv). Inset: Plot of emission intensity (λ_{em} = 543 nm) versus Na_2S concentration. (d) Emission spectra of *trans*-**3** (20 μM, λ_{ex} = 424 nm, in CH_3CN/H_2O (4:1, v/v)) upon addition of increasing concentrations of Na_2S (0 to 140.0 equiv). Inset: Plot of emission intensity (λ_{em} =489 nm) versus Na_2S concentration.

10. Emission interference experiments of *trans*-3 and *cis*-3 toward CN^- ions.

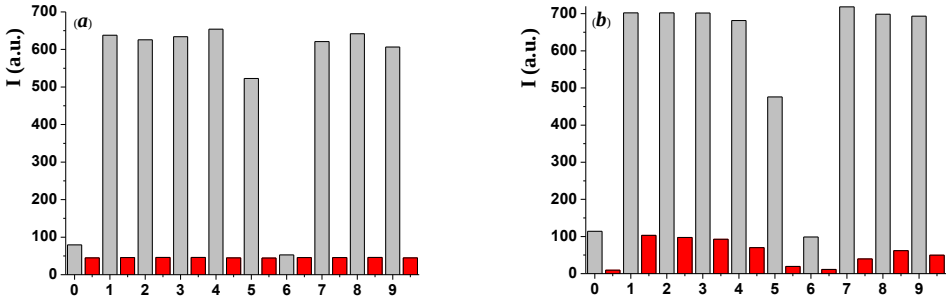

Figure S16. (*a*) Fluorescence spectra of probe *cis*-**3** (20 μM) in presence of various anion (2.3 equiv.) in CH_3CN solution n. The gray bars represent the emission at 536 nm in the presence of 2.3 equiv. of the anion of interest (form 0 to 9: *cis*-**3** only, F^-, Cl^-, Br^-, I^-, HSO_4^-, $H_2PO_4^-$, AcO^-, BF_4^-, NO_3^-, ClO_4^-). The red bars indicate the change that occurs upon subsequent addition of 2.3 equiv. of CN^- to the solution containing *cis*-**3** and the anion of interest; (*b*) Fluorescence spectra of probe *trans*-**3** (20 μM) in presence of various anion (2.0 equiv.) in CH_3CN solution. The gray bars represent the emission at 478 nm in the presence of 2.0 equiv. of the anion of interest (form 0 to 9: *trans*-**3** only, F^-, Cl^-, Br^-, I^-, HSO_4^-, $H_2PO_4^-$, AcO^-, BF_4^-, NO_3^-, ClO_4^-). The red bars indicate the change that occurs upon subsequent addition of 2.0 equiv. of CN^- to the soluteion containing *trans*-**3** and the anion of interest.

11. Emission spectra of titration of *cis*-3 and *trans*-3 with CN^- in CH_3CN.

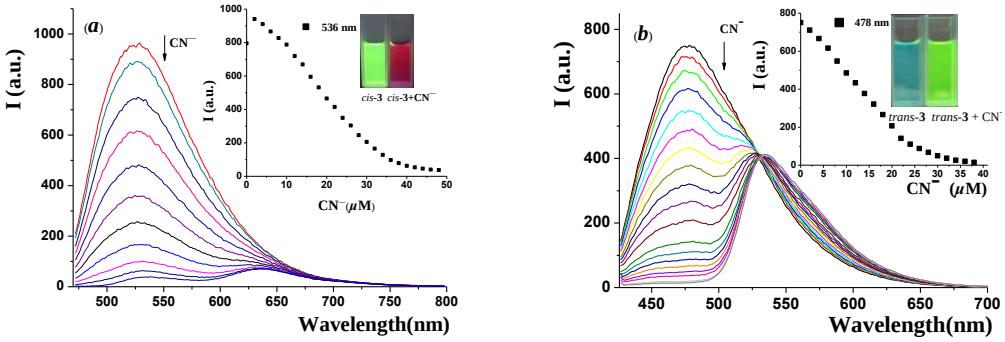

Figure S17. (*a*) Emission spectra of *cis*-**3** (20 μM, λ_{ex} =461 nm, in CH_3CN) upon addition of increasing concentrations of CN^- (as its TBA salt, 0 to 2.3 equiv). Inset: Plot of emission intensity (λ_{em} = 536 nm) versus TBACN concentration. (*b*) Emission spectra of *trans*-**3** (20 μM, λ_{ex} = 424

nm, in CH_3CN) upon addition of increasing concentrations of CN^- (as its TBA salt, 0 to 2.0 equiv). Inset: Plot of emission intensity (λ_{em} =478 nm) versus TBACN concentration.

12. The fluorescence detection limit of *tran*-3 and *cis*-3 with CN^- in CH_3CN-H_2O solution.

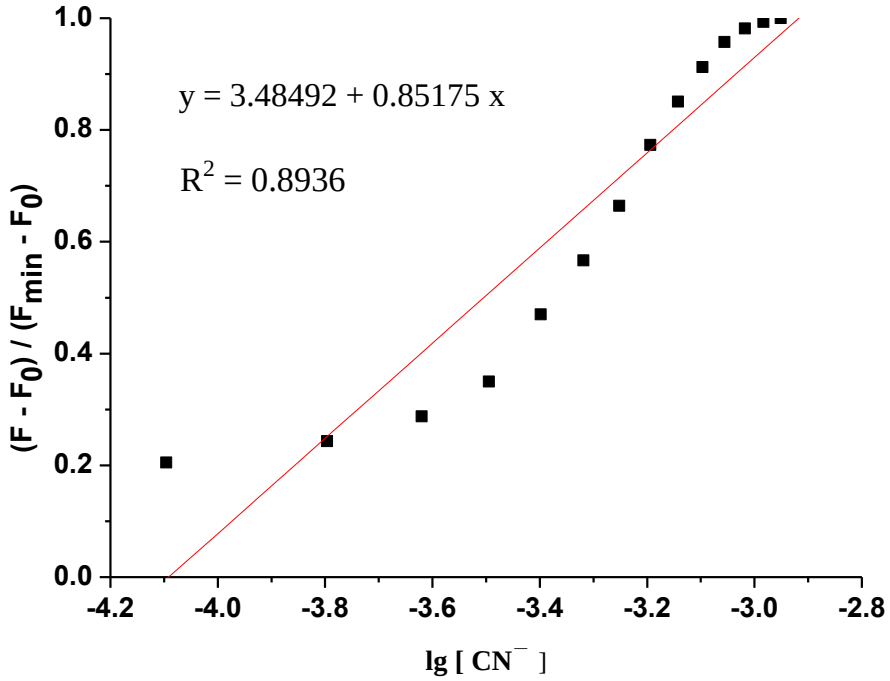

Figure S18. Emission intensity ratio (F_{543}) of *cis*-**3** (20 μM) as a function of CN^- concentration from 0-1120 μM (0–56 equiv) in in CH_3CN/H_2O (9:1, v/v).

Equiation	Y = A + B * X	
Parameter	Value	Error
A	3.48249	0.28258
B	0.851753	0.08480
R	SD	N
0.94532	0.10278	14

The result of the analysis as follows:

Linear Equation: Y = 3.48249+0.851753* X, R^2 = 0.8936

S= 0.851753 * 10^6, K = 3, δ = 0.10278

LOD = K *δ / S = 0.362 μM

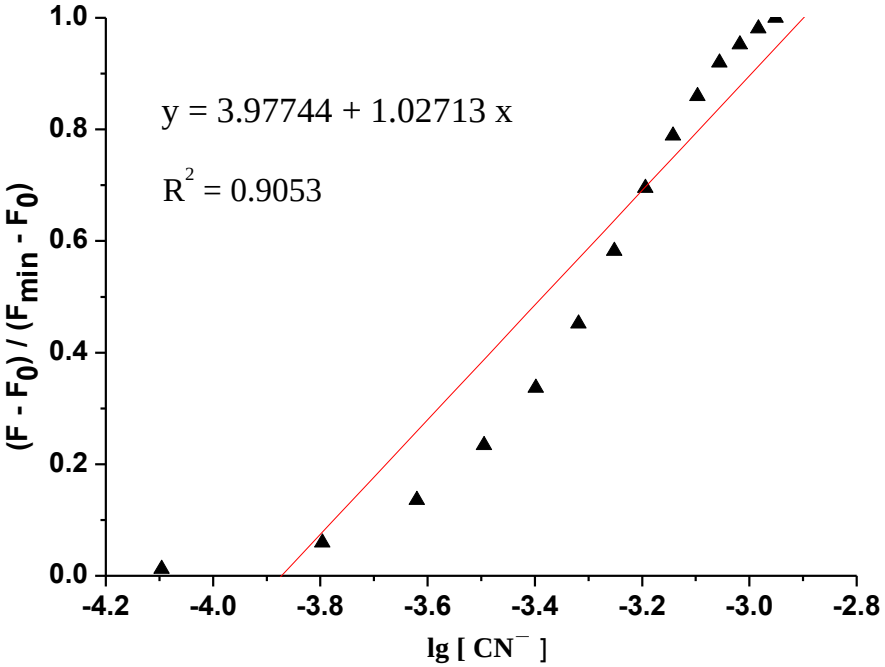

Figure S19. Emission intensity ratio (F_{489}) of *trans*-**3** (20 μM) as a function of CN^- concentration from 0-1120 μM (0–56 equiv) in in CH_3CN/H_2O (4:1, v/v).

Equiation	Y = A + B * X	
Parameter	Value	Error
A	3.97744	0.31953
B	1.02713	0.09592
R	SD	N
0.95145	0.11622	14

The result of the analysis as follows:

Linear Equation: Y = 3.97744+1.02713* X, R^2 = 0.9053

S= 1.02713 * 10^6, K = 3, δ = 0.11622

LOD = K *δ / S = 0.339 μM

13. ^{1}H NMR titration spectra of isomer 3 with TBACN

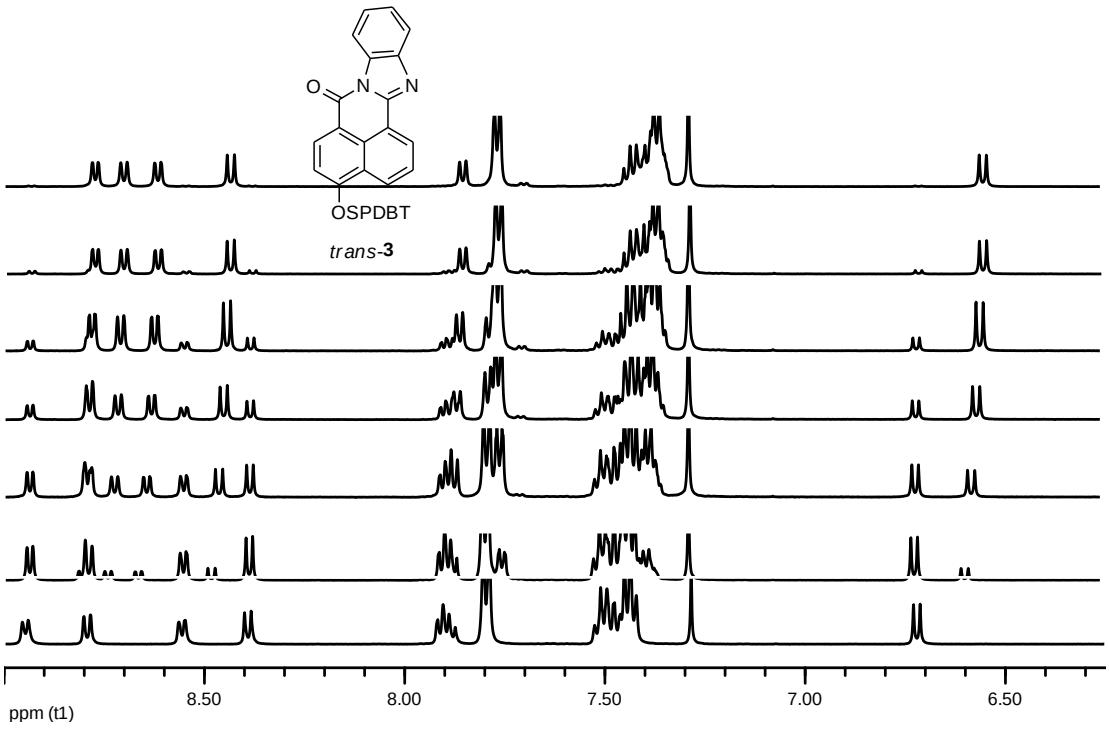

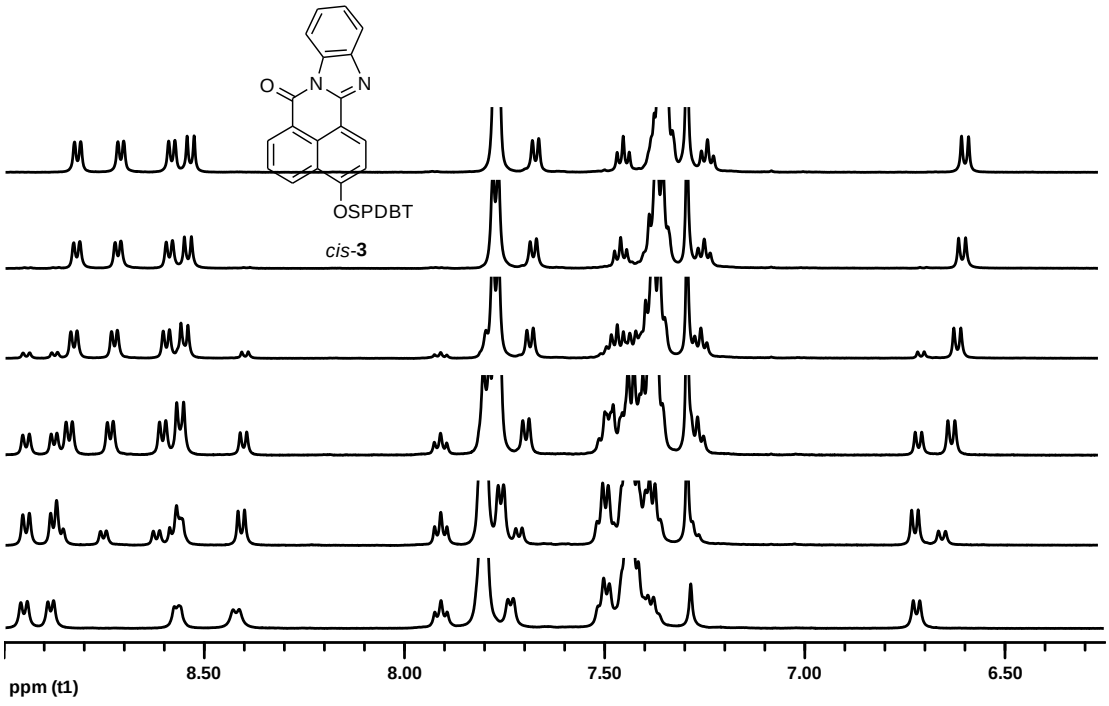

Figure S20. ^{1}H NMR titration spectra of *trans*-**3** (top, 1.92 × 10^{-2} mol /L) and *cis*-**3** (bottom, 3.8 × 10^{-2} mol /L) in $CDCl_3$ upon addition of TBACN (in $CDCl_3$), from the bottom to top: 0, 0.32, 0.64, 0.96, 1.28, 1.60 equiv. (*trans*-**3**) and 0, 0.52, 1.04, 1.56, 2.08, 2.60 equiv. (*cis*-**3**).

14. The final state of ^{1}H NMR titration spectra of isomer 3 with TBACN

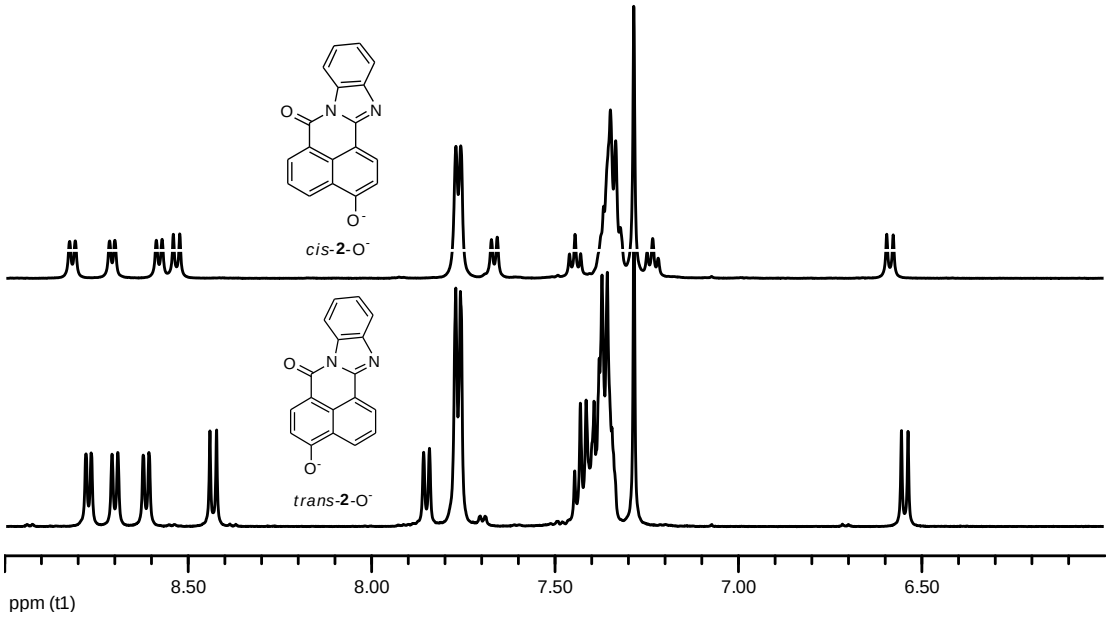

Figure S21. The final state of ^{1}H NMR titration spectra of *trans*-**3** and *cis*-**3** in $CDCl_3$ upon addition of CN^- ions

15. The fluoride interference experiments on the test paper

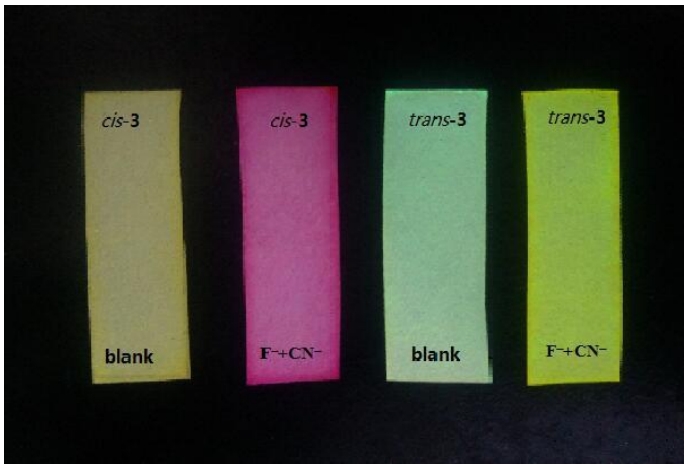

Figure S22. The fluorescence changes of the test papers of *trans*-**3** and *cis*-**3** (1.0 mmol/L-1) with the mixed anions of CN^- and F^- (both 5.0 mmol/L-1), the test strips were irradiated with a hand-held UV lamp at 365 nm.